Supplementary material for LHCb-PAPER-2016-052

Figure 1 shows the signal mass resolution as a function of $m(\chi)$. It is obtained from the simulation and is scaled to the resolution observed in data for $J/\psi \to \mu^+\mu^-$ decays from the normalization channel, where the scaling factor corresponds to $\sigma^{\rm DATA}_{J/\psi\to\mu^+\mu^-}/\sigma^{\rm MC}_{J/\psi\to\mu^+\mu^-} = 1.167$. The resolution is then interpolated in the entire mass range using cubic splines.

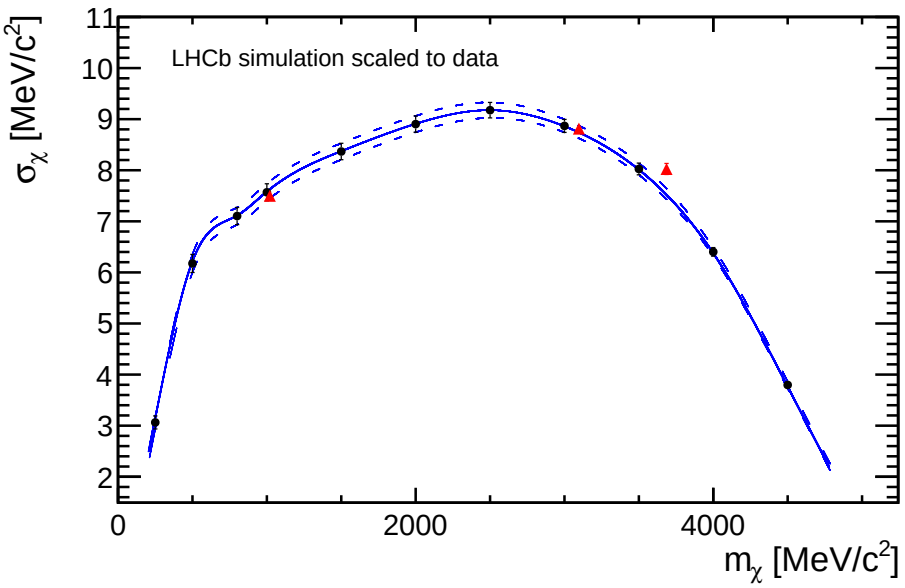

Figure 1: Signal mass resolution as a function of $m(\chi)$. The black points show the resolution obtained from the simulation and scaled to the $J/\psi \to \mu^+\mu^-$ resolution observed in data; the red triangles show the resolution observed in data for $\phi \to \mu^+\mu^-$, $J/\psi \to \mu^+\mu^-$ and $\psi(2S) \to \mu^+\mu^-$ decays. The signal resolution is interpolated using cubic splines: the central value is plotted with the solid blue line, while the error band is indicated by the two dashed blue lines.

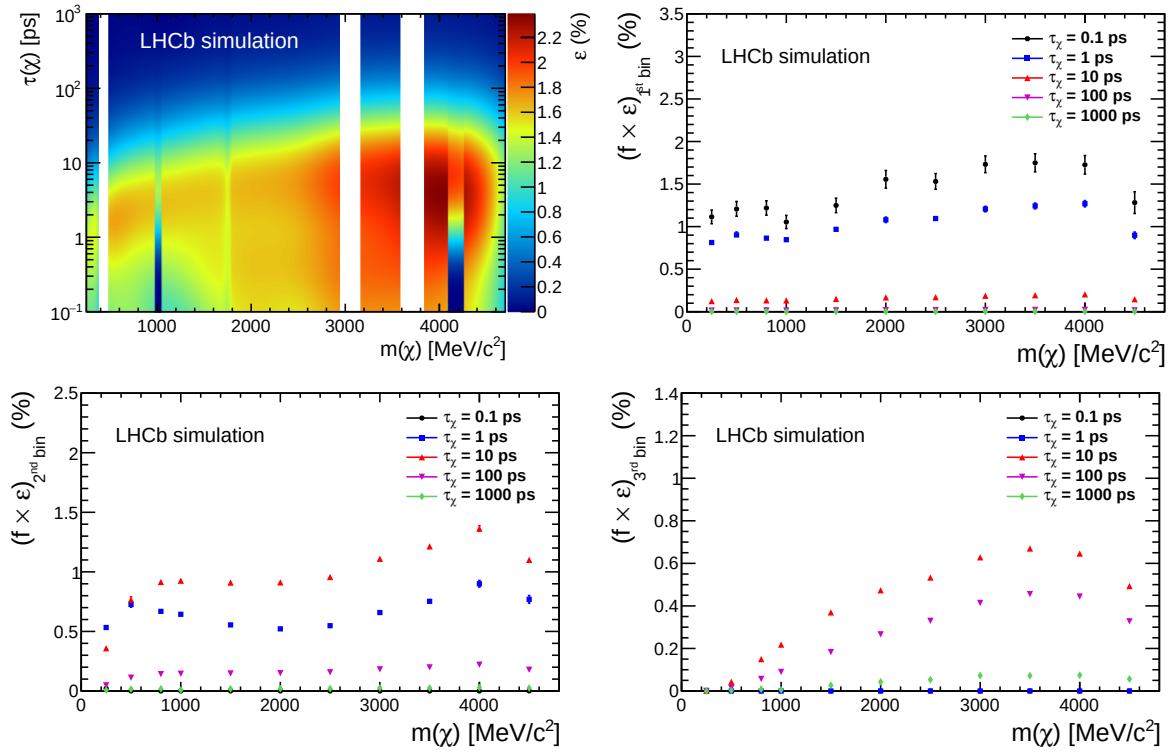

Figure 2: Top left: total efficiency as a function of the signal mass and lifetime. Fully-vetoed regions corresponding to the K^0_S, J/ψ, $\psi(2S)$ and $\psi(3770)$ are excluded from the plot. The vetoes which are applied in the prompt decay-time region of the ϕ and $\psi(4160)$ result in a drop of the efficiency at low lifetime. The structure around 1.8 GeV/c^2 corresponds to the additional particle identification requirements applied around the D^0 mass. Top right and bottom: contribution of each decay-time region to the total signal efficiency for several lifetime hypotheses as a function of mass. The plots show the product of the fraction of events in each decay-time region and the corresponding efficiency. Values are obtained from the simulation before applying any of the ϕ, K^0_S, J/ψ, $\psi(2S)$, $\psi(2S)$, $\psi(3770)$ and $\psi(4160)$ vetoes.

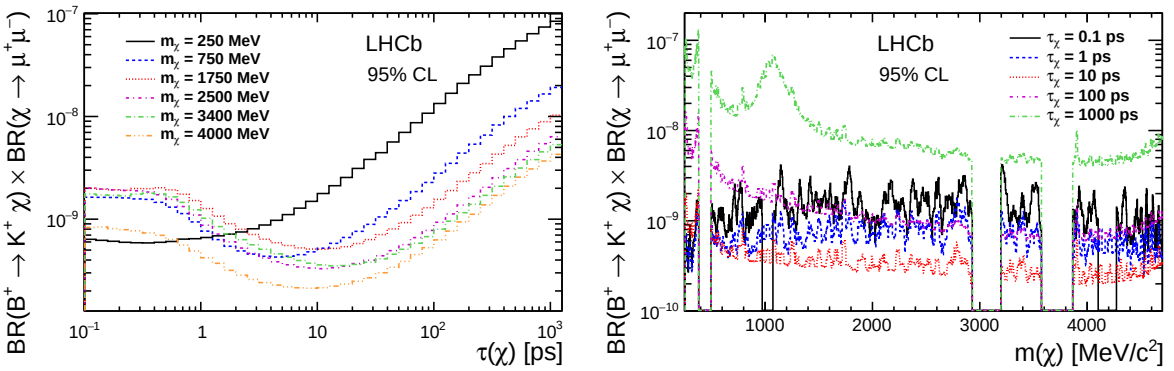

Figure 3: Excluded branching fraction for the $B^+ \to K^+\chi(\mu^+\mu^-)$ decay at the 95% CL for (left) several mass and (right) lifetime hypotheses. Regions corresponding to the fully-vetoed K^0_S, J/ψ, $\psi(2S)$ and $\psi(3770)$ and to the partially-vetoed ϕ and $\psi(4160)$ are excluded from the figure.

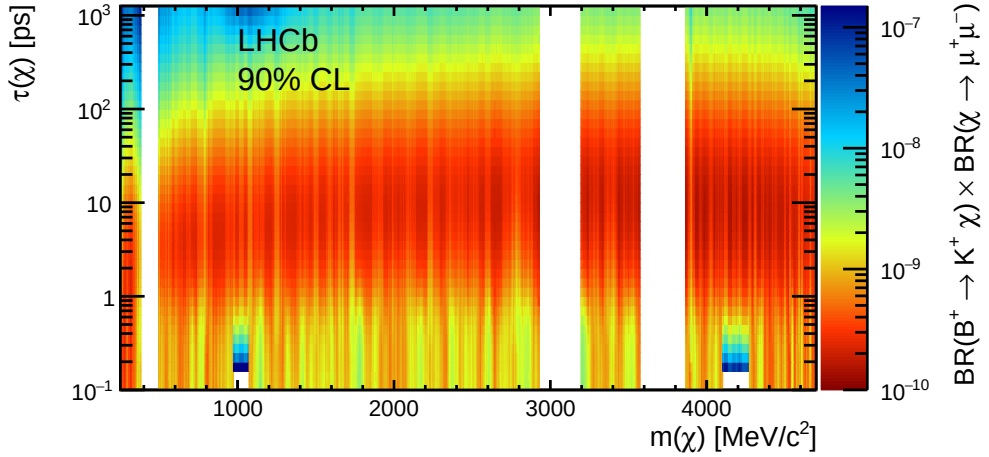

Figure 4: Excluded branching fraction for the $B^+ \to K^+\chi(\mu^+\mu^-)$ decay as a function of $m(\chi)$ and $\tau(\chi)$ at 90% CL. Regions corresponding to the fully-vetoed K^0_S, J/ψ, $\psi(2S)$ and $\psi(3770)$ and to the partially-vetoed ϕ and $\psi(4160)$ are excluded from the figure. All systematic uncertainties are included in the calculation of the upper limit.

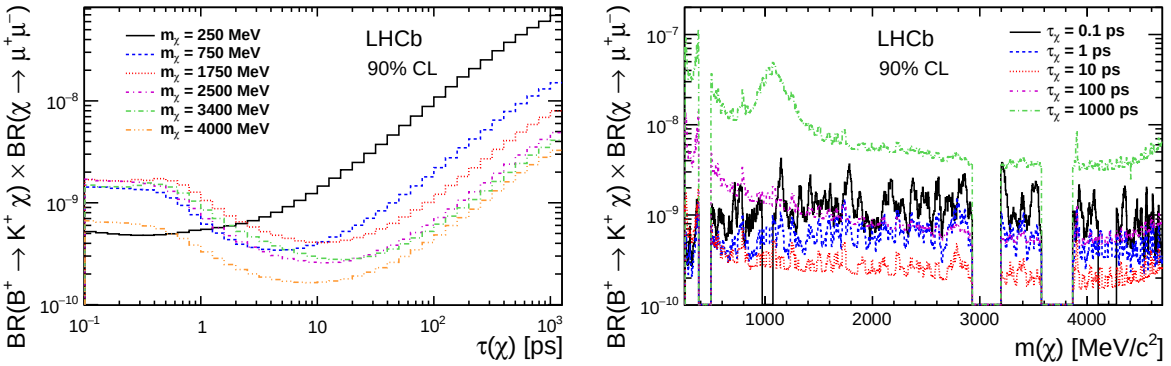

Figure 5: Excluded branching fraction for the $B^+ \to K^+\chi(\mu^+\mu^-)$ decay at the 90% CL for (left) several mass and (right) lifetime hypotheses. Regions corresponding to the fully-vetoed K^0_S, J/ψ, $\psi(2S)$ and $\psi(3770)$ and to the partially-vetoed ϕ and $\psi(4160)$ are excluded from the figure.

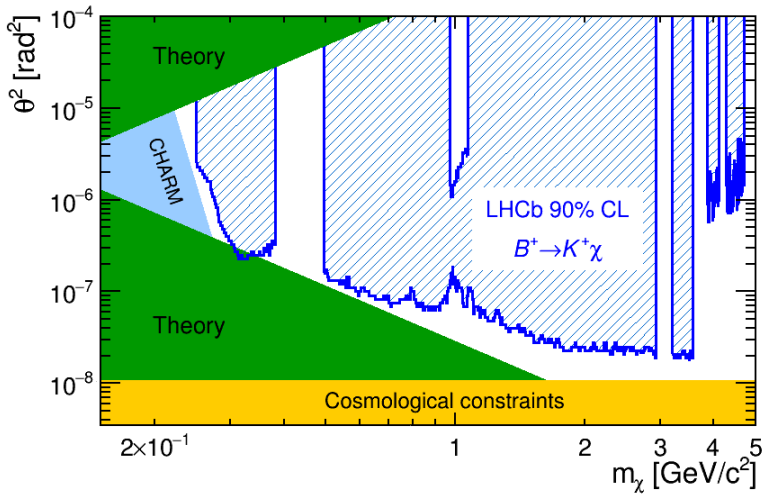

Figure 6: Parameter space of the inflaton model described in Refs. [1–3]. The region excluded at 90% CL by this analysis is shown by the blue hatched area. Direct experimental constraints set by the CHARM experiment [4] and regions forbidden by theory or cosmological constraints [3] are also shown.

References

[1] B. Batell, M. Pospelov, and A. Ritz, *Multi-lepton signatures of a hidden sector in rare B decays*, Phys. Rev. **D83** (2011) 054005, arXiv:0911.4938.

[2] F. Bezrukov and D. Gorbunov, *Light inflaton hunter's guide*, JHEP **05** (2010) 010, arXiv:0912.0390.

[3] F. Bezrukov and D. Gorbunov, *Light inflaton after LHC8 and WMAP9 results*, JHEP **07** (2013) 140, arXiv:1303.4395.

[4] CHARM collaboration, F. Bergsma *et al.*, *Search for axion like particle production in 400 GeV proton-copper interactions*, Phys. Lett. **B157** (1985) 458.